Chinese Journal of Aeronautics, 2013,26(3): 554–562

Chinese Society of Aeronautics and Astronautics
& Beihang University

Chinese Journal of Aeronautics

cja@buaa.edu.cn
www.sciencedirect.com

Hybrid calibration method for six-component force/torque transducers of wind tunnel balance based on support vector machines

Ma Yingkun, Xie Shilin *, Zhang Xinong, Luo Yajun

State Key Laboratory for Strength and Vibration of Mechanical Structures, School of Aerospace, Xi'an Jiaotong University, Xi'an 710049, China

Received 3 September 2012; revised 18 October 2012; accepted 11 December 2012
Available online 15 May 2013

KEYWORDS

Hybrid;
Multi-dimensional;
Nonlinear coupling;
Support vector machines;
Transducers

Abstract A hybrid calibration approach based on support vector machines (SVM) is proposed to characterize nonlinear cross coupling of multi-dimensional transducer. It is difficult to identify these unknown nonlinearities and crosstalk just with a single conventional calibration approach. In this paper, a hybrid model comprising calibration matrix and SVM model for calibrating linearity and nonlinearity respectively is built up. The calibration matrix is determined by linear artificial neural network (ANN), and the SVM is used to compensate for the nonlinear cross coupling among each dimension. A simulation of the calibration of a multi-dimensional sensor is conducted by the SVM hybrid calibration method, which is then utilized to calibrate a six-component force/torque transducer of wind tunnel balance. From the calibrating results, it can be indicated that the SVM hybrid calibration method has improved the calibration accuracy significantly without increasing data samples, compared with calibration matrix. Moreover, with the calibration matrix, the hybrid model can provide a basis for the design of transducers.

1. Introduction

Six-component force/torque transducer system is a multi-dimensional sensor which is able to measure all the force and torque components of an arbitrary six-component force system. Since it can measure the whole force information of a structure joint, six-component force/torque transducers have covered a wide range of applications in force measurement of rocket engine test, vehicle wheels experiments, robot wrist and some related automatic systems.[1–3] Typical wind tunnel balance is a six-component force/torque transducer, capable of measuring an aerodynamic normal force, axial force, side force, yawing moment, pitching moment and rolling moment by monitoring structural deformation with strain gages.[4] Despite the fact that lots of novel ideas and careful considerations[5–7] were made in designing, manufacturing and using transducers, the crosstalk is unavoidable and complicated; in addition, the error of measurement system, the interference of external environment and the aging of sensor components

* Corresponding author. Tel.: +86 29 82668483.
E-mail addresses: mayk.123@stu.xjtu.edu.cn (Y. Ma), slxie@mail.xjtu.edu.cn (S. Xie).

Peer review under responsibility of Editorial Committe of CJA.

1000-9361
http://dx.doi.org/10.1016/j.cja.2013.04.056

are all uncertain actually. These factors cause the relationship between the actual output signal and the applied loads to be complicated nonlinearity. In order to improve the measuring accuracy, it is necessary to calibrate the transducer for a practical relationship.

Conventional calibration methods involve parametric identification process through regression analysis on the basis of a presumed model. As one of the traditional calibration methods, least-square optimization method has been extensively applied for calibration of multi-dimensional sensors.[8] This approach is difficult for its requirement of large number of experimental data, however the calibration experiment is a demanding task. In order to avoid this pitfall, Refs.[5–7] calibrated the sensors based on the simulation of finite element method (FEM) analysis. Gao et al.[9] derived a hyper static multi-component torque sensor's calibration matrix using the designing principles and theories of anisotropic elasticity and piezoelectricity. It can be obtained the coupling level and the relationship between every single output signal and the respective input load from the calibration matrix, which can be used as a basis to improve the design of sensors consequently. Liang et al.[10] designed an decoupling configuration for the force sensor and then calibrated it based on artificial neural network (ANN). After network training, the weight value of ANN is taken as the decoupling calibration matrix. These approaches mentioned above are employed by the following hypothesis and principle of the sensor: (A) the deformation of elastic body and Wheatstone bridge circuits are linear; (B) the sensor is self-decoupled, which means that there is no distinct cross coupling between components.

Therefore, the actual relationships between output signals and the applied loads are such complicated nonlinear that cannot be characterized by calibration matrix no matter how many testing data are considered.

As a non-parametric method, ANN can approximate any nonlinear function with arbitrary accuracy, so Schultz[11] employed ANN to calibrate quartz crystal pressure sensors. This ANN modeling is practically a pure black-box method, that is, to model the relationship of the sensor only relying on the input and output data regardless of any priori system knowledge. This pure black-box ANN model generally has such disadvantages as long training cycle, large network scale, requirement of a large number of training data and poor generalization performance.[12–14] Masri[15] proposed the concept of hybrid ANN modeling, which combines the knowledge-based model with the ANN model so as to reduce network scale and training cycle, and improve the accuracy and generalization. Cao[16] applied the approach to model the dynamics of friction component in brake system of vehicle transmission, where ANN was used to describe the nonlinear relationships among oil pressure, temperature and rotation speed. The results showed outstanding predicting accuracy and generalization performance.

Support vector machines (SVM) is a kind of machine-learning tool developed by Vapnik.[17] It implements the structural risk minimization (SRM) principle to solve the nonlinear and high dimension problems with small sample set. Different from ANN, SVM is based on the SRM principle which makes SVM achieve optimum networks structure, so that the solution of SVM is unique and globally optimal. SVM provides an effective novel non-parametric approach to achieve global optimum due to these attractive features and empirical performance.[14,18–21]

Consequently, in order to take advantage of hybrid modeling concept and SVM, this paper develops an SVM hybrid calibration method which consists of traditional method and SVM method for calibrating linearity and nonlinearity of six-component force/torque transducer respectively. The rest of the paper is organized in the following manner. Section 2 presents background theory regarding SVM. Section 3 gives a brief introduction to the procedure of the hybrid calibration. Section 4 applies this approach to a calibration simulation and in Section 5 it is applied to a six-component force/torque transducer calibration experiments. Finally, Section 6 closes with some concluding remarks.

2. Support vector machines

Support vector machine was developed by Vapnik[17] for solving problem of pattern recognition, and then a generalization of SVM for regression problem was proposed. With the introduction of ε-insensitive loss function, a nonlinear regression estimation problem is constructed according to the principle of structural risk minimization. Given a set of training data points, $\{(\boldsymbol{x}_1,y_1), (\boldsymbol{x}_2,y_2),\ldots,(\boldsymbol{x}_n,y_n)\}\in \mathbf{R}^n\times\mathbf{R}$, such that $\boldsymbol{x}_i$ is an input and y_i is a target output. SVM approximates the linear regression function $g(\boldsymbol{x})$ given by

$$g(\boldsymbol{x}) = \boldsymbol{w}\boldsymbol{x} + b \tag{1}$$

where $\boldsymbol{w}$ is the weighting vector, b the bias of output. The primal optimization problem is

$$\min\{\frac{1}{2}\|\boldsymbol{w}\|^2 + C\sum_{i=1}^{N}(\xi_i+\xi_i^*)$$
$$\text{s.t.}\begin{cases}(\boldsymbol{w}^{\mathrm{T}}\boldsymbol{x}_i+b)-y_i\leqslant\varepsilon+\xi_i\\ y_i-(\boldsymbol{w}^{\mathrm{T}}\boldsymbol{x}_i+b)\leqslant\varepsilon+\xi_i^*\\ \xi_i,\xi_i^*\geqslant 0, i=1,2,\cdots,N\end{cases} \tag{2}$$

where ξ_i and ξ_i^* are positive slack variables, C is the penalty coefficient which determines the trades-off between the empirical risk and the regularization term, ε the insensitive parameter. For nonlinear regression, the input vectors are mapped to a high-dimensional feature space, where an optimal decision hyper plane is constructed. We write the Lagrange function so as to get its saddle points, and then the value of $\boldsymbol{w}$ can be substituted and simplify to get the corresponding dual problem of Eq. (2). As a convex quadratic programming problem, one can deal with feature space of arbitrary dimensionality without knowing how to map explicitly. Given that kernels function $K(\boldsymbol{x}_i, \boldsymbol{x}_j)$ equals the inner product of two vectors $\boldsymbol{x}_i$ and $\boldsymbol{x}_j$ in the feature space, the nonlinear quadratic programming problem takes the form:

$$\min\{\varepsilon\sum_{i=1}^{l}(a_i+a_i^*)-\sum_{i=1}^{l}y_i(a_i-a_i^*)+\frac{1}{2}\sum_{i,j=1}^{l}(a_i-a_i^*)(a_j-a_j^*)K(\boldsymbol{x}_i,\boldsymbol{x}_j)\}$$
$$\text{s.t.}\begin{cases}\sum_{i=1}^{l}(a_i-a_i^*)=0\\ a_i,a_i^*\in[0,C]\end{cases} \tag{3}$$

where a_i and a_i^* are Lagrange multipliers. Support vectors are the only elements of the data points that are used in determining Eq. (3) as the coefficients $(a_i-a_i^*)$ of other data points are all zero.[14]

The corresponding decision function model can be represented as

$$g(\boldsymbol{x}) = \sum_{i=1}^{l}(a_i - a_i^*)K(\boldsymbol{x}_i, \boldsymbol{x}) + b \tag{4}$$

where $b = y_j - \sum y_i a_i K(\boldsymbol{x}_i, \boldsymbol{x}_j)$, and the kernel function $K(\cdot)$ can be any symmetric function satisfying Mercer's condition.[22] Typical example is the use of a radial basis function (RBF) kernel $K(\boldsymbol{x}_i, \boldsymbol{x}_j) = \exp(-\gamma|\boldsymbol{x}_i - \boldsymbol{x}_j|^2)$, which is used in this paper.

It can be seen from the theory that SVM transforms the nonlinear problem to a linear problem in a higher dimensional feature space, thus the computational complexity of nonlinear problem is significantly reduced.

The training process is equivalent to solving a linear quadratic programming, which makes the solution of SVM unique and globally optimal.

SVM implements the SRM principle to minimize the upper bound of the generalization error rather than minimize the training error. Accordingly, SVM can achieve an optimal generalization performance by striking a right balance between empirical error and confidence interval to solve the nonlinear and high dimensional problem with small sample set.

The model of SVM is actually a matrix of support vectors $(a_i - a_i^*)$. The configuration is brief for calibration.

Therefore, SVM is considered to provide an effective approach to calibrate the nonlinear relationship of multi-dimensional sensor.

3. SVM hybrid calibration method

For a linear system or a nonlinear system just with simple structure style, it could be accurate enough to calibrate it with empirical knowledge utilizing first principle computation and conventional parameter identification method. It is referred to as knowledge-based model. For a complex nonlinear system, this approach may cost lots of time while its accuracy is still unsatisfied. Even though the knowledge-based model may be coarse, it can reflect the primary characteristics of system. The non-parametric modeling methods, for instance ANN and SVM can approximate an arbitrary nonlinear system, but they model the overall behavior of system only relying on the input and output data, regardless of any priori knowledge. In this study, a non-parametric modeling method, such as SVM is employed to complement the knowledge-based model so as to reduce the calibration errors.

The objective of calibration is to model the relationship between the input loads and the output signals, which can be expressed as

$$\boldsymbol{z} = f(\boldsymbol{u}) \tag{5}$$

where $\boldsymbol{z} \in \mathbf{R}^m$ denotes the applied loads of m dimensions, and $\boldsymbol{u} \in \mathbf{R}^n$ denotes the sensor output signal of n dimensions, $f(\cdot)$ represents the functional relationship of multi-dimensional sensor which is generally complex nonlinear as mentioned previously. In order to model $f(\cdot)$ exactly, Eq. (5) is rewritten as

$$\boldsymbol{z}^* = f_1(\boldsymbol{u}) + f_2(\boldsymbol{u}) \tag{6}$$

where $\boldsymbol{z}^* \in \mathbf{R}^m$ denotes the predicted value of $\boldsymbol{z}$, $f(\cdot)$ is expressed as the summation of two parts: $f_1(\cdot)$ and $f_2(\cdot)$, $f_1(\cdot)$ represents the knowledge-based model which describes the linear primary input–output characteristics of sensor. It is easy to identify $f_1(\cdot)$ according to priori knowledge using aforementioned methods. $f_2(\cdot)$ reflects the residual between the knowledge-based model $f_1(\cdot)$ and the actual loads to be measured. It represents nonlinear properties of sensors which is hard to determine with traditional approach. Thus, SVM is used to identify $f_2(\cdot)$. Input to SVM is the output signals u of n dimensions, and the output to SVM is an approximation of the unknown residual $f_2(\cdot)$. The SVM hybrid calibration method is utilized to determine $f_1(\cdot)$ and $f_2(\cdot)$ respectively, and the scheme of procedure is illustrated as Fig. 1. There are two parameters while using SVM: C and γ, which are the key to the accuracy of forecasting. In the training process, the SVM parameters γ and C should be determined firstly in the following steps:

(1) For multivariate d-dimensional problems, the RBF kernel parameter χ is set as $\chi^d \in (0.1, 0.5)$,[23] where $1/(2\chi^2) = \gamma$. Cherkassky and Ma[24] validated that such values can yield SVM performance good enough within a range of various regression data sets.
(2) Cherkassky and Ma[24] also clarified the penalty coefficient C obtained from the training data then becomes $C = \max(|y^* + 3\sigma_y|, |y^* - 3\sigma_y|)$, where y^* and σ_y are the mean and the standard deviation of the training data output values respectively. The training data will be pre-normalized to be zero mean and unit deviation, therefore the C maintains 3.

4. Sensor calibration simulation

For calibrating a multi-dimensional sensor, the traditional method is to fit a large number of sample data to determine the calibration matrix based on the assumption of linear cross coupling between each components, nevertheless the nonlinear coupling form is unknown commonly, therefore, calibration of this nonlinearity with non-parametric modeling approach is necessary.

This section simulates an SVM hybrid calibration of a simple dummy multi-dimensional sensor, describes the calibration process and compares the results with other methods to evaluate its comprehensive performance. For instance, given a 2-D input, 2-D output sensor, and the relationship between input and output signal is as follows:

$$\boldsymbol{P} = \boldsymbol{C}\boldsymbol{U} + e(\boldsymbol{u}) \tag{7}$$

where the applied loads $\boldsymbol{P} = [p_1 \ p_2]^{\mathrm{T}}$, the output signals $\boldsymbol{U} = [u_1 \ u_2]^{\mathrm{T}}$, $\boldsymbol{C}$ is the calibration matrix, and $e(\boldsymbol{u})$ the nonlinear coupling term. It is assumed that this sensor's actual relationship takes the form of

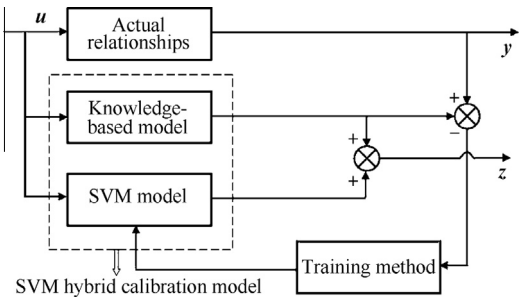

Fig. 1 Schemes of SVM hybrid calibration.

$$\boldsymbol{C} = \begin{bmatrix} c_{11} & c_{12} \\ c_{21} & c_{22} \end{bmatrix} = \begin{bmatrix} 120 & 1 \\ 8 & 140 \end{bmatrix}$$
$$e(u) = \begin{Bmatrix} e_1(u) \\ e_2(u) \end{Bmatrix} = \begin{Bmatrix} 0.8u_1u_2^2 \\ 0.5u_1^2u_2 \end{Bmatrix} \quad (8)$$

The output signals $u_1 \in [0, 5]$ V, $u_2 \in [0, 5]$ V. Given 20 groups of random distribution data (u_1, u_2), and the sample data set is obtained according to Eqs. (7) and (8). Ignoring nonlinear coupling, the relationship between input and output can be described as

$$\boldsymbol{P}^* = \boldsymbol{C}^* \boldsymbol{U} \quad (9)$$

where $\boldsymbol{P}^*$ is the predicted value of $\boldsymbol{P}$, $\boldsymbol{C}^*$ the predicted value of $\boldsymbol{C}$. According to Eq. (9), utilize least square fitting of sample set to obtain the map matrix[25] as

$$\boldsymbol{C}^* = \begin{bmatrix} 120.74 & 8.5 \\ 10.71 & 142.15 \end{bmatrix} \quad (10)$$

With the known $\boldsymbol{C}^*$ and output signal $u_1, u_2 \in [0, 5]$ V, the output-input relation surface according to Eq. (7) can be obtained, and then it was compared with the actual curve achieved through Eq. (11) as shown in Fig. 2. It can be seen from the result that there are obvious errors especially in high amplitude areas. The root-mean-square errors (RMSE) of two channels' calibration result with map matrix are 15.530 and 9.931. From the simulation process, we found that increasing samples could not reduce the RMSE efficiently.

The fitting result $\boldsymbol{C}^*\boldsymbol{U}$ is knowledge-based model, as $f_1(u)$, then model the residual with SVM:

(1) Choose the output voltage signal $\boldsymbol{U}$ as input of training sample and the residual between actual value and calibration matrix predicted value as output of training sample. Training sample set is composed of 20 groups of random-distribution applied loads and their respective output signals.
(2) Determine the coefficient γ and C then train the sample data to acquire the SVM model.
(3) Combine the knowledge-based model and SVM model together to get hybrid model for multi-input multi-output (MIMO) sensor.

With output signal $u_1, u_2 \in [0,5]$V, the output-input relation curve can be obtained according to the hybrid model as shown in Fig. 3 and the corresponding RMSEs are 1.255 and 1.073, respectively. Compared with Fig. 2, the curves predicted by hybrid model are more consistent with actual curves than the ones determined by calibration matrix, and the accuracy is improved significantly.

In addition, the authors use pure SVM to calibrate this sensor: choose the output voltage signal $\boldsymbol{U}$ as input of training sample and measured loads $\boldsymbol{P}$ as output of training sample, then train these sample data to acquire the SVM-based black box model, then calibrate the sensor to obtain its output-input relation surface as shown in Fig. 4 and the RMSEs are 11.890 and 15.620 respectively. The performance of pure SVM-based black box model deteriorates for larger measured loads. It can be seen from the result that with a small number of sample data, calibrating a sensor only with neither least square fitting nor SVM-based black box can reach satisfactory accuracy, while SVM hybrid method can improve the accuracy significantly.

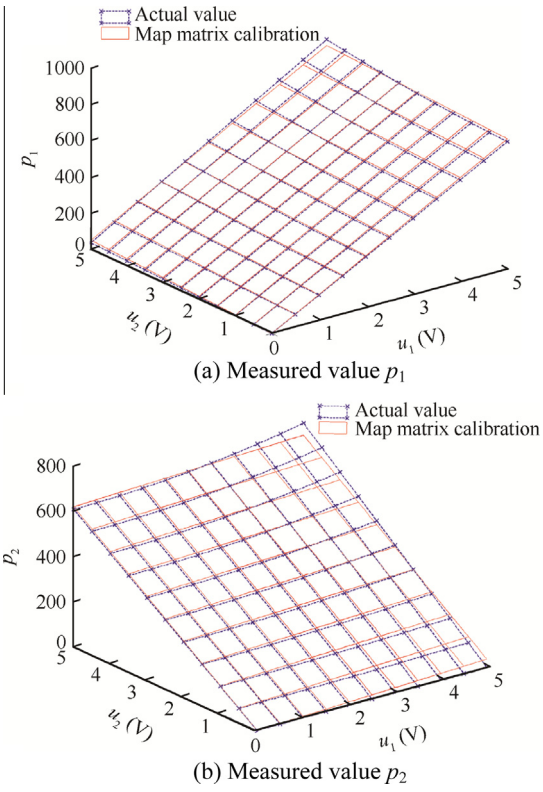

Fig. 2 Results of two channels predicted with calibration matrix compared with true values.

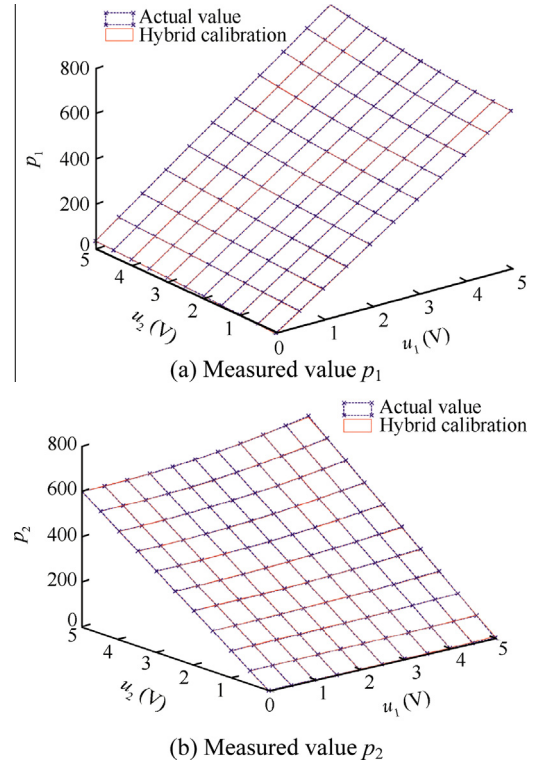

Fig. 3 Results of two channels predicted with SVM hybrid method compared with true values.

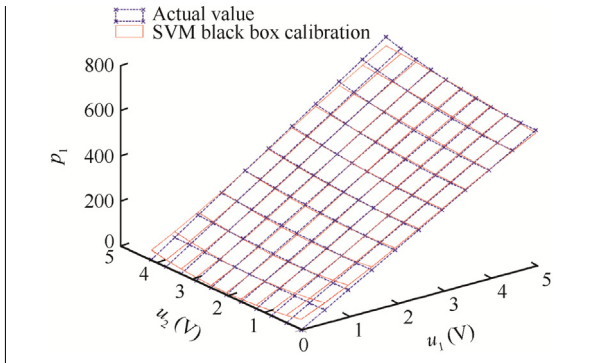

(a) Measured value p_1

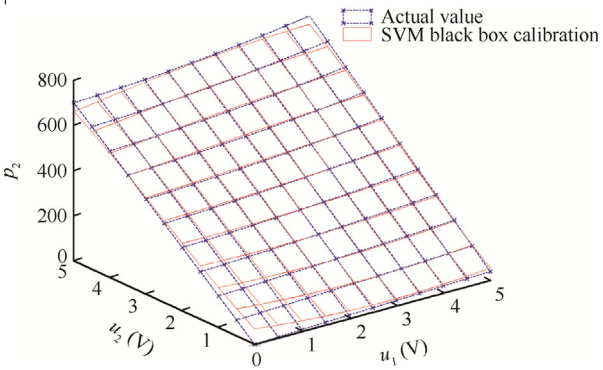

(b) Measured value p_2

Fig. 4 Results of two channels predicted with pure black-box SVM compared with true values.

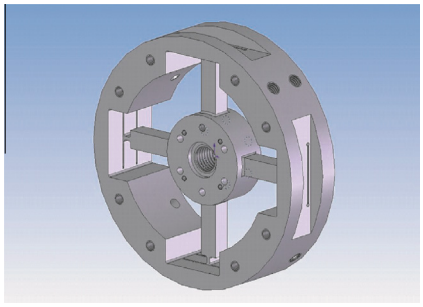

Fig. 5 Sketch of cross-beamed transducer.

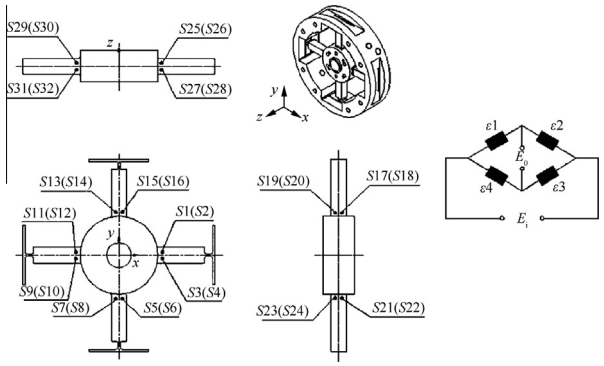

Fig. 6 Strain gauges position and bridge diagram.

5. Calibration experiments

With the method described in Section 3, this section is concerned with the calibration of a cross-beamed six-component force/torque transducer system for wind tunnel balance.

In this six-component force measurement system, the force-sensing elements are strain gauges. The measurement system is a cross-beamed structure shown as Fig. 5. The frame center is connected to specimen. The force or torque is transmitted through the four beams to exterior circle which is cut into straight beams. The force level can be obtained by measuring the elastic deformation of the main beams. The material of frame is stainless steel (2Cr13), and the specification is shown in Table 1. The carrying capacity is $F_x = F_y = F_z = 800$ N, $M_z = 450$ N·m, $M_x = M_y = 465$ N·m. F_x, F_y and F_z denote the component forces in x, y and z directions, M_x, M_y and M_z denote the component torques in x, y and z directions. There are eight Wheatstone bridges composed of 32 strain gauges, whose locations are shown as Fig. 6. The "S" in Fig. 6 points the position of the strain gauges on the cross-beamed structure, ε1-ε4 denote the pattern of Wheatstone bridges, E_o and E_i denote the output voltage and the input voltage of bridge respectively.

5.1. Calibration experiments

The equipment for static calibration experiments is a 500 kN universal testing machine CMT5000 whose force control accuracy is 1%. The force/torque vector to be measured is $\boldsymbol{F} = [F_x\ F_y\ F_z\ M_x\ M_y\ M_z]^{\mathrm{T}}$, and the output voltage signal is $\boldsymbol{U} = [u_1\ u_2\ \ldots\ u_8]^{\mathrm{T}}$. According to calibration principle, this paper designed six groups of linearly independent single load: each force F_x, F_y and F_z are loaded up to 800 kN and then unloaded in chronological sequence with fixed step (100 N); the torque M_x and M_y are loaded up to 465 N·m and then unloaded respectively with fixed step (93 N·m); the torque M_z is loaded up to 450 N·m and then unloaded with fixed step (90 N·m). Each force/torque component is loaded and unloaded individually. The loading fixtures of the F_x, F_z M_x and M_z are shown as Fig. 7.

At each step, the load values and the eight output voltage values are recorded, and accordingly 78 groups of calibration data are obtained. The linear part of the sensor's output-input relationship can be expressed as $\boldsymbol{F}_1 = \boldsymbol{CU}$, where $\boldsymbol{F}_1$ is the linear part of $\boldsymbol{F}$, and

Table 1 Specification of cross-beamed frame.

Dimension	Length	Width	Height	Center diameter	Circle diameter
Internal beam	30	10	10	50	140
External beam	38	2	10	50	140

Note: unit: mm.

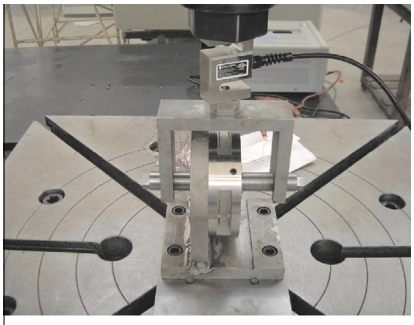

(a) Loading fixture of the F_x component

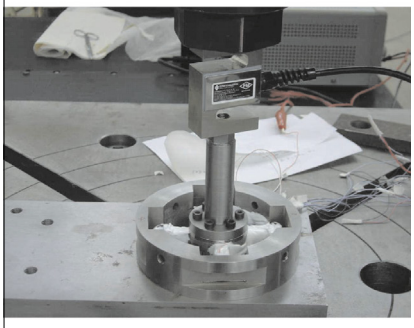

(b) Loading fixture of the F_z component

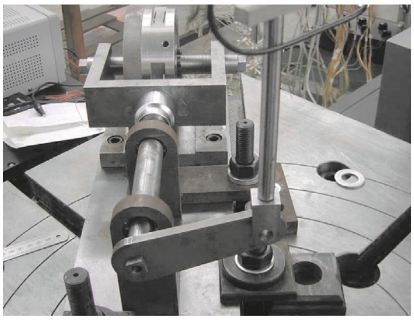

(c) Loading fixture of the M_x component

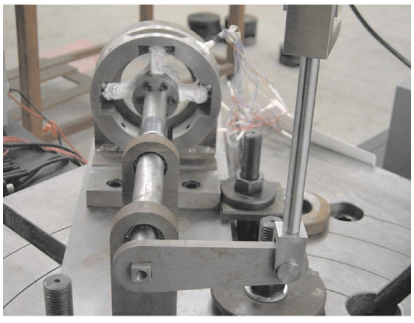

(d) Loading fixture of the M_z component

Fig. 7 Loading fixtures in six-axis force/torque sensor calibration test.

$$\begin{bmatrix} F_x \\ F_y \\ F_z \\ M_x \\ M_y \\ M_z \end{bmatrix} = \begin{bmatrix} c_{11} & c_{12} & \cdots & c_{18} \\ c_{21} & c_{22} & \cdots & c_{28} \\ \vdots & \vdots & \vdots & \vdots \\ c_{61} & c_{62} & \cdots & c_{68} \end{bmatrix} \begin{bmatrix} u_1 \\ u_2 \\ \vdots \\ u_8 \end{bmatrix} \tag{11}$$

According to the SVM hybrid calibration approach described previously, first, acquire the elements of the map matrix $\boldsymbol{C}$, then predict the residual by SVM, and finally combine them together to accomplish the hybrid calibration model.

5.2. Identification of calibration matrix

The calibration matrix can be obtained by linear ANN[10] as shown in Fig. 8, V_1–V_8 are the input channels of the linear ANN. The input vector $\boldsymbol{U} = [u_1\ u_2\ \ldots\ u_8]^{\mathrm{T}}$ is the output voltages of the sensitive bridge circuits, and the output vector $\boldsymbol{F} = [F_x\ F_y\ F_z\ M_x\ M_y\ M_z]^{\mathrm{T}}$ is the forces/torques applied on the sensor. The learning samples are the 78 groups of calibration data. After network training, the weight value $\boldsymbol{W} = [w_{ij}]$ ($i = 1,2,\ldots,6$; $j = 1,2,\ldots,8$) is taken as the calibration matrix of Eq. (11). The matrix is shown as

$$\boldsymbol{C} = \begin{bmatrix} -132.78 & 327.26 & -96.68 & -42.81 & -54.64 & 63.24 & -44.74 & 25.13 \\ -413.51 & 574.37 & -736.58 & 530.468 & 133.07 & -138.92 & 100.01 & -128.41 \\ 155.18 & -140.09 & 129.89 & -126.36 & -255.72 & 31.86 & -254.66 & 26.64 \\ 426.63 & -378.75 & 340.67 & -335.86 & -457.22 & 402.23 & -436.05 & 500.45 \\ -748.68 & 710.62 & -671.65 & 685.98 & 388.99 & -324.86 & 245.04 & -326.02 \\ 233.94 & -75.55 & 210.38 & -55.64 & -94.38 & 104.37 & -100.96 & 90.12 \end{bmatrix} \tag{12}$$

With the known $\boldsymbol{C}$ and output voltage, the measured load components at every load step in each programmed loading–unloading mode can be obtained from Eq. (11). To evaluate the accuracy of the model, the computed load components are illustrated in Fig. 9 with respect to load step number for six loading–unloading modes. Note that in Fig. 9, the applied load component in each mode is plotted in the upper part, and the crosstalk load components in each mode are plotted in the lower part. It can be seen from Fig. 9 that when each single force/torque component is applied, the other load components predicted by calibration matrix differ significantly from the actual value which should be zero. It means that between each channels, there are nonlinear coupling which cannot be predicted by linear calibration matrix, no matter how much sample data there is. Because of coupling nonlinearity, the other channels also have output signals. The coupling level can be obtained from the calibration matrix, and the signals of these channels are generally complicated nonlinearity.

5.3. SVM hybrid calibration method

SVM hybrid calibration method is applied to calibrating the six-component force/torque sensor. According to the approach

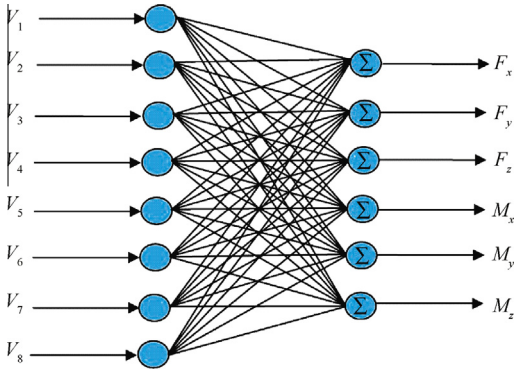

Fig. 8 ANN model for calibration matrix.

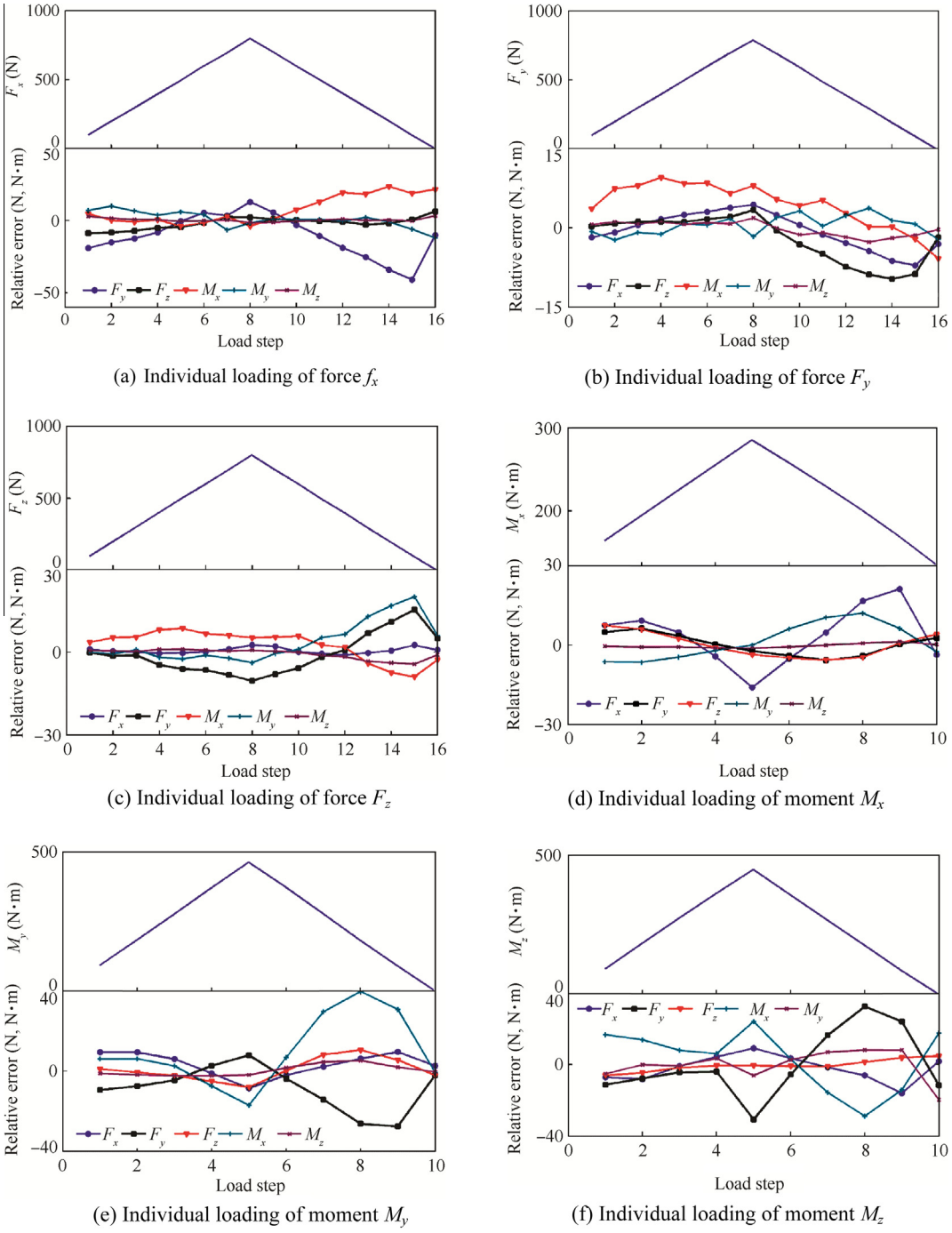

Fig. 9 Predicted results of single load with calibration matrix.

described previously, the calibration matrix $\boldsymbol{C}$ acquired in Section 5.2 is chosen as knowledge-based model, and the nonlinear cross coupling part is predicted by SVM. Choose the output voltage signal $\boldsymbol{U}$ as input of training set and the residual between actual value and predicted value through calibration matrix as output of training set which is composed of 78 groups of measured data. Train the sample set to obtain its SVM model. Combine the knowledge-based model and SVM model together to obtain the hybrid model of this six-component force/torque sensor. The sequence of six component forces is predicted with the SVM hybrid calibration method as shown in Fig. 10.

It can be seen from Fig. 10 that when only one single component force, namely F_x is applied, the curve predicted by hybrid model almost corresponds with the actual curve where F_x follows the load process curve, and the other component forces maintain almost zero. At all the other steps, errors are always at a low level as well.

There are two types of indexes we defined to evaluate the calibration precision of multi-component force/torque sensors, which characterize the measuring error and the interference error respectively. Type I = max (|Load value – measured value|)/full-scale value; Type II = max (|measured value of the other dimension|)/the full-scale value of one dimension. Table 2

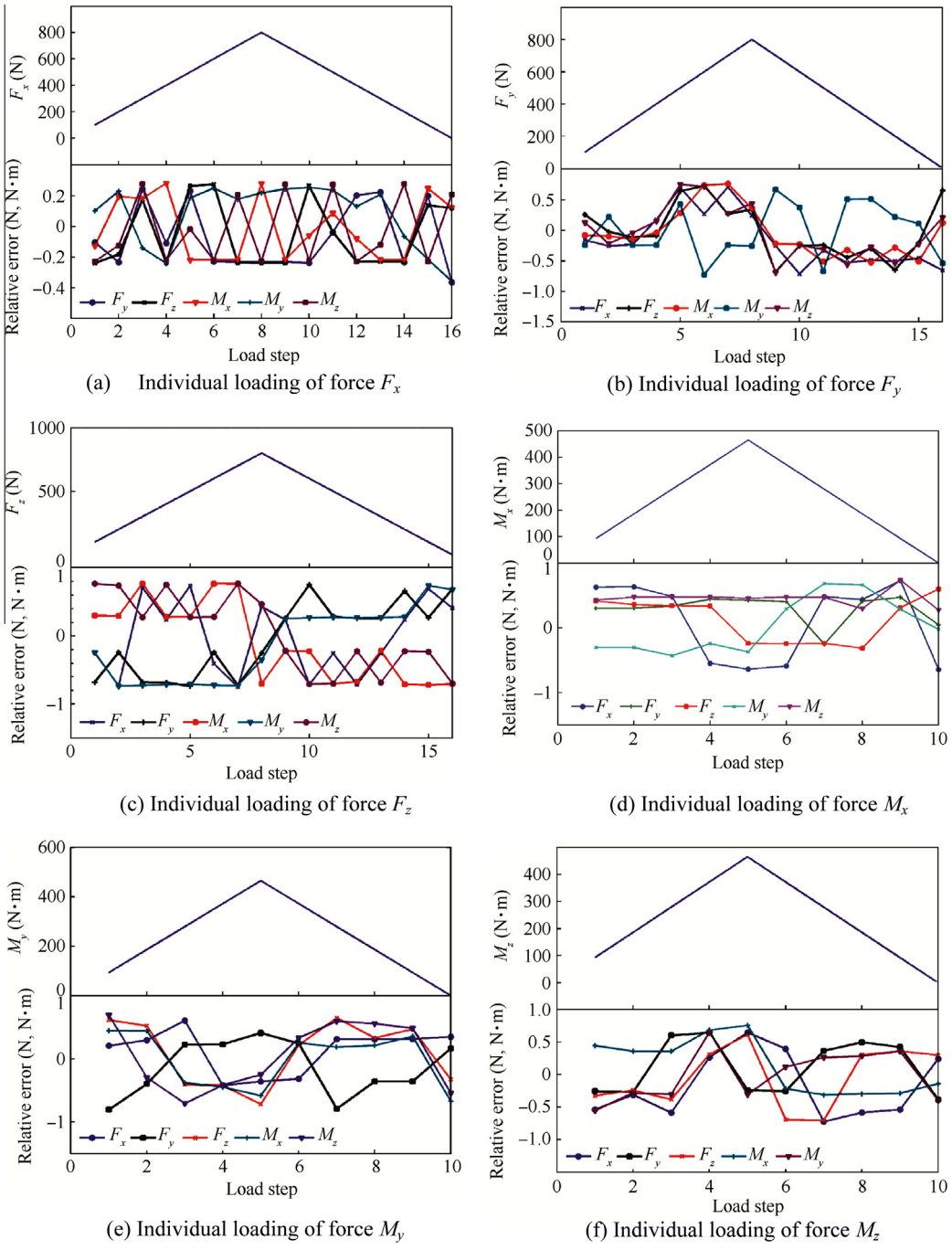

Fig. 10 Predicted results of single load with SVM hybrid method.

Table 2 Comparison of calibration errors between conventional approach and SVM hybrid method in two types.

Component force	Error of Type I (%)		Error of Type II (%)	
	Calibration matrix	SVM hybrid	Calibration matrix	SVM hybrid
F_x	0.6	0.04	2.7	0.03
F_y	1.4	0.08	5.1	0.09
F_z	0.6	0.09	1.3	0.09
M_x	3.6	0.05	8.5	0.08
M_y	0.7	0.08	4.3	0.10
M_z	1.1	0.09	1.2	0.08

gives the comparison of calibration precision between the traditional method (calibration matrix model) and hybrid SVM calibration method in terms of Type I and Type II errors of six load components.

From Fig. 10 and Table 2, all of the errors are less than 0.1%. Compared with the approach proposed by Xie et al.,[26] this SVM hybrid calibration method can compensate for nonlinear coupling between each dimension more exactly and efficiently. Therefore, it can be said the calibration accuracy was improved significantly with the same amount of sample data. Moreover, unlike ANN, the SVM training process did not contain any iteration procedure, thus it is a time-saving method relatively.

6. Conclusions and outlook

(1) Compared with traditional calibration approach, SVM hybrid calibration method can efficiently compensate for nonlinear cross coupling among each dimension without increasing sample data, and may improve the calibration accuracy significantly with all of the errors less than 0.1%.
(2) SVM hybrid model consists of knowledge-based model; therefore, compared with pure black box model of SVM, SVM hybrid model not only performances higher precision and better generalization, but also reflects the level of linear cross coupling. Accordingly, SVM hybrid model can provide a basis for the design of sensors. With the advantages over the other machine learning method, this hybrid approach based on SVM is also a more time-saving method relatively.
(3) In conclusion, the SVM hybrid approach provides an effective way for MIMO sensor calibration. This method can also be used to calibrate dynamic characteristics of MIMO sensors, which will be studied in the future work.

Acknowledgements

This work is co-supported by National Science Foundation of China (Grant No. 10772142), National Natural Science Key Foundation of China (Grant No. 10832002), and the Fundamental Research Funds for the Central Universities.

References

1. Diddens D, Reynaerts D, Van Brussel H. Design of a ring-shaped three-axis micro force/torque sensor. *Sens Actuators, A* 1995;**46**(1–3):225–32.
2. Liu SA, Tzo HL. A novel six-component force sensor of good measurement isotropy and sensitivities. *Sens Actuators, A* 2002;**100**(2–3):223–30.
3. Canbay E, Ersoy U, Tankut T. A three component force transducer for reinforced concrete structural testing. *Eng Struct* 2004;**26**(2):257–65.
4. Johnson TH, Parker PA, Landman D. Calibration modeling of nonmonolithic wind-tunnel force balances. *J Aircr* 2010;**47**(6):1860–6.
5. Jia ZY, Lin S, Liu W. Measurement method of six-axis load sharing based on the Stewart platform. *Measurement* 2010;**43**(3):329–35.
6. Song AG, Wu J, Qin G, Huang WY. A novel self-decoupled four degree-of-freedom wrist force/torque sensor. *Measurement* 2007;**40**(9–10):883–91.
7. Li YJ, Sun BY, Zhang J, Qian M, Jia ZY. A novel parallel piezoelectric six-axis heavy force/torque sensor. *Measurement* 2009;**42**(5):730–6.
8. Beyeler F, Muntwyler S, Nelson BJ. Design and calibration of a microfabricated 6-axis force-torque sensor for microrobotic applications. *IEEE Int Conf Robot Automation (ICRA)* 2009;520–5.
9. Gao CY, Li WQ, Sun BY. Research on the piezoelectric torsional effect of a rectangular quartz disc and a novel drilling dynamometer. *Measurement* 2010;**43**(3):336–43.
10. Liang QK, Zhang D, Song QJ, Ge YJ, Cao HB, Ge Y. Design and fabrication of a six-dimensional wrist force/torque sensor based on E-type membranes compared to cross beams. *Measurement* 2010;**43**(10):1702–19.
11. Schultz RL. Dynamic neural network calibration of quartz transducers. *Int J Robust Nonlin* 2002;**12**(11):1053–66.
12. Hou YL, Yao JT, Zeng DX, Chen J, Zhao YS. Development and calibration of a hyperstatic six-component force/torque sensor. *Chin J Mech Eng* 2009;**22**(4):505–13.
13. Cao M, Wang KW, Fujii Y, Tobler WE. A hybrid neural network approach for the development of friction component dynamic model. *J Dyn Syst-T Asme* 2004;**126**(1):144–53.
14. Dong YF, Li YM, Lai M, Xiao MK. Nonlinear structural response prediction based on support vector machines. *J Sound Vib* 2008;**311**(3–5):886–97.
15. Masri SF. A hybrid parametric nonparametric approach for the identification of nonlinear-systems. *Probabilist Eng Mech* 1994;**9**(1–2):47–57.
16. Cao LJ. Support vector machines experts for time series forecasting. *Neurocomputing* 2003;**51**:321–39.
17. Vapnik VN. *The nature of statistical learning theory*. New York: Springer; 1999.
18. Ubeyli ED. Least squares support vector machine employing model-based methods coefficients for analysis of EEG signals. *Exp Syst Appl* 2010;**37**(1):233–9.
19. Wu Q. Power load forecasts based on hybrid PSO with Gaussian and adaptive mutation and Wv-SVM. *Exp Syst Appl* 2010;**37**(1):194–201.
20. Wu Q, Law R. An intelligent forecasting model based on robust wavelet v-support vector machine. *Exp Syst Appl* 2011;**38**(5):4851–9.
21. Guo Z, Bai G. Application of least squares support vector machine for regression to reliability analysis. *Chin J Aeronaut* 2009;**22**(2):160–6.
22. Boser BE, Guyon IM, Vapnik VN. A training algorithm for optimal margin classifiers. *Proceedings of the fifth annual ACM workshop on computational learning theory*; 1992. p. 144–52.
23. Cao ZK, Han H, Gu B. Modeling of variable speed refrigerated display cabinets based on adaptive support vector machine. *Mech Syst Signal Pr* 2010;**24**(1):78–89.
24. Cherkassky V, Ma YQ. Practical selection of SVM parameters and noise estimation for SVM regression. *Neural Networks* 2004;**17**(1):113–26.
25. Hong WC. Hybrid evolutionary algorithms in a SVR-based electric load forecasting model. *Int J Elec Power* 2009;**31**(7–8):409–17.
26. Xie SL, Zhang XN, Chen SL, Zhu CC. Hybrid neural network models of transducers. *Meas Sci Technol* 2011;**22**(10):105201.

Ma Yingkun received B.S. degree from Xi'an Jiaotong University in 2007, and then became a Ph.D. candidate there. His main research interest is modeling of dynamic systems.

Xie Shilin received B.S. and Ph.D. degrees from Xi'an Jiaotong University in 1993 and 1999, respectively, and then became a teacher there. His main research interests are modeling of dynamic systems and vibration control.